doi:10.1093/jmcb/mjw029
Published online August 17, 2016

Article

BDNF rescues prefrontal dysfunction elicited by pyramidal neuron-specific DTNBP1 deletion *in vivo*

Wen Zhang[1], Kathryn M. Daly[1], Bo Liang[1], Lifeng Zhang[1], Xuan Li[1], Yun Li[1,*], and Da-Ting Lin[1,2,3,*]

[1] Intramural Research Program, National Institute on Drug Abuse, National Institutes of Health, 333 Cassell Drive, Baltimore, MD 21224, USA
[2] The Jackson Laboratory, 600 Main Street, Bar Harbor, ME 04609, USA
[3] The Solomon H. Snyder Department of Neuroscience, Johns Hopkins University School of Medicine, 725 N. Wolfe Street, Baltimore, MD 21205, USA
* Correspondence to: Yun Li, E-mail: yunlijax@gmail.com; Da-Ting Lin, E-mail: lind3@mail.nih.gov

Dystrobrevin-binding protein 1* (*Dtnbp1*) is one of the earliest identified schizophrenia susceptibility genes. Reduced expression of DTNBP1 is commonly found in brain areas of schizophrenic patients. *Dtnbp1*-null mutant mice exhibit abnormalities in behaviors and impairments in neuronal activities. However, how diminished DTNBP1 expression contributes to clinical relevant features of schizophrenia remains to be illustrated. Here, using a conditional *Dtnbp1* knockout mouse line, we identified an *in vivo* schizophrenia-relevant function of DTNBP1 in pyramidal neurons of the medial prefrontal cortex (mPFC). We demonstrated that DTNBP1 elimination specifically in pyramidal neurons of the mPFC impaired mouse pre-pulse inhibition (PPI) behavior and reduced perisomatic GABAergic synapses. We further revealed that loss of DTNBP1 in pyramidal neurons diminished activity-dependent secretion of brain-derived neurotrophic factor (BDNF). Finally, we showed that chronic BDNF infusion in the mPFC fully rescued both GABAergic synaptic dysfunction and PPI behavioral deficit induced by DTNBP1 elimination from pyramidal neurons. Our findings highlight brain region- and cell type-specific functions of DTNBP1 in the pathogenesis of schizophrenia, and underscore BDNF restoration as a potential therapeutic strategy for schizophrenia.

Keywords: schizophrenia, GABAergic, disinhibition, PFC, BDNF, *Dtnbp1*

Introduction

Schizophrenia is a severe and chronic psychiatric disorder, affecting ~1% of the general population (Regier et al., 1993). Both genetic and environmental risk factors contribute to its etiology (Schmitt et al., 2014). Recent genetic studies have identified a substantial number of schizophrenia-associated genes (Purcell et al., 2014; Schizophrenia Working Group of the Psychiatric Genomics, 2014; Stefansson et al., 2014). However, the pathophysiology of schizophrenia is still unclear and current pharmacological treatments are often of limited success (Lieberman et al., 2005). Identifying pathogenic mechanisms of schizophrenia is critical for developing effective therapeutic strategies.

Dystrobrevin-binding protein 1 (*Dtnbp1*) is one of the earliest identified schizophrenia susceptibility genes (Straub et al., 2002). Over the years, the association between *Dtnbp1* genetic variations with schizophrenia is under debate (Talbot, 2009; Farrell et al., 2015), with negative reports (Sanders et al., 2008; Sullivan et al., 2008), as well as confirmations from diverse population (Duan et al., 2007; Allen et al., 2008; Sun et al., 2008; Vilella et al., 2008). Nevertheless, reduced DTNBP1 levels have been commonly found in brain areas (e.g. dorsolateral prefrontal cortex and hippocampus) of schizophrenic patients (Talbot et al., 2004; Weickert et al., 2008), regardless of whether the patients are carriers for *Dtnbp1* mutations. Notably, a recent publication showed that diminished expression levels of disrupted-in-schizophrenia 1, another schizophrenia-associated gene, led to DTNBP1 reduction (Lee et al., 2015). This finding raises an interesting possibility that reduced DTNBP1 expression represents a common pathogenic mechanism for schizophrenia.

Previous studies from a spontaneous loss-of-function *Dtnbp1* mutant mouse line (*Sandy* or *Dtnbp1*^{sdy} mice) showed that homozygous *Dtnbp1*^{sdy} mice displayed various schizophrenia-relevant behavioral deficits, including reduced pre-pulse inhibition (PPI), reduced spatial memory and reduced social interactions (Talbot, 2009; Papaleo et al., 2012). Using the *Dtnbp1*^{sdy} mice, multiple roles of DTNBP1 in the regulation of neurotransmission pathways were proposed, including alterations in membrane levels of dopamine and glutamate receptors, reduction in glutamate release and

Received April 26, 2016. Revised May 12, 2016. Accepted May 16, 2016.

diminished activity of GABAergic interneurons (Li et al., 2003; Chen et al., 2008; Ji et al., 2009; Tang et al., 2009; Carlson et al., 2011). It is likely that DTNBP1 plays distinct roles in different brain regions and neuronal types to regulate the above-mentioned neurotransmission pathways. Therefore, unraveling DTNBP1 function in a brain region- and neuronal type-specific fashions will greatly facilitate illuminating the pathological mechanism by which DTNBP1 reduction contributes to schizophrenia. However, in the existing *Dtnbp1*^{sdy} mouse model, *Dtnbp1* is globally eliminated from embryonic stage and throughout adulthood, making it impossible to unravel brain region- and cell type-specific functions of DTNBP1. Therefore, development of new mouse models allowing spatial- and temporal-specific manipulations of DTNBP1 level will greatly facilitate the understanding of DTNBP1 function in schizophrenia.

Among all identified psychiatric risk factors, brain-derived neurotrophic factor (BDNF) might be one of the most important molecules for maintaining normal brain function. BDNF participates in various essential neurobiological pathways such as neurogenesis and neuroplasticity (Barde et al., 1982; Ghosh et al., 1994; Lu, 2003). Clinical studies have shown that patients with schizophrenia or depressive disorders exhibited low levels of BDNF in the CNS and blood serum (Karege et al., 2002; Dwivedi et al., 2003; Weickert et al., 2003; Kim et al., 2007; Green et al., 2011; Martinotti et al., 2012). In addition, genetic variations in *BDNF* have also been associated with psychiatric disorders (Szekeres et al., 2003; Gratacos et al., 2007). A recent publication from Yuan et al. (2015) demonstrated an *in vitro* link between these two psychiatric risk factors: DTNBP1 deletion reduced BDNF exocytosis in pyramidal neurons. However, the work by Yuan et al. (2015) employed RNA interference technique to diminish DTNBP1 expression, which lacked the specificity to target particular neuronal population. Several important questions remain to be addressed: (i) whether cell type-specific DTNBP1 deletion *in vivo* from pyramidal neurons would induce any schizophrenia-relevant behavioral deficits; (ii) whether *in vivo* loss of DTNBP1 specifically in pyramidal neurons would lead to similar abnormal synaptic transmission as observed *in vitro*; and (iii) whether BDNF application *in vivo* would fully rescue the synaptic and behavior deficits induced by loss of DTNBP1.

The present study aimed to address the above questions using a newly developed mouse strain harboring a conditional knockout allele for *Dtnbp1*. Our results revealed that loss of DTNBP1 in pyramidal neurons in the medial prefrontal cortex (mPFC) induced behavioral abnormity and disrupted GABAergic transmission. We further demonstrated that loss of DTNBP1 in pyramidal neurons reduced activity-dependent BDNF secretion. Finally, we showed that restoration of extracellular BDNF in the mPFC *in vivo* fully rescued GABAergic dysfunction and behavioral deficit induced by DTNBP1 elimination from mPFC pyramidal neurons. Our results highlight the *in vivo* connection between the two psychiatric risk factors DTNBP1 and BDNF, and underscore BDNF restoration as a promising therapeutic strategy for schizophrenia.

Results

Eliminating DTNBP1 in adult mPFC elicited reduced PPI

To study cell type-specific functions of DTNBP1, we obtained embryonic stem cells from The European Conditional Mouse Mutagenesis Program (Skarnes et al., 2011), and generated a 'knockout-first conditional-ready' *Dtnbp1* mouse strain (Figure 1A). The targeting cassette contained mouse *En2* splice acceptor, an IRES::*lacZ* trapping element, and a floxed promoter-driven *neo* element inserted into introns of *Dtnbp1* gene. Therefore, the originally developed mouse strain was a *Dtnbp1* knockout line carrying *Dtnbp1* gene-targeting *LacZ* element to reflect the endogenous *Dtnbp1* expression. High levels of DTNBP1 expression were observed in layers II/III and V of cerebral cortex (Figure 1B). After Flipase (Flp) removal of the *lacZ* element, the targeting cassette was converted to a true *Dtnbp1* conditional allele, that Cre recombinase would eliminate the floxed exon 5 to induce a frame-shift mutation and subsequent degradation of DTNBP1.

We obtained homozygous *Dtnbp1*$^{F/F}$ mice and first verified Cre-dependent DTNBP1 knockout efficiency by western blotting using *in vitro* cultured hippocampal neurons from *Dtnbp1*$^{F/F}$ embryos (Figure 1C). We infected neuronal cultures with an adeno-associated virus (AAV-Cre-eGFP) expressing Cre-eGFP fusion protein under a CaMKII promoter. Seven days after Cre viral infection, DTNBP1 protein levels were notably reduced in hippocampal cultures. To further validate *in vivo* Cre-mediated DTNBP1 knockout efficiency, we focally injected the same virus into the mPFC of 6–8-week-old *Dtnbp1*$^{F/F}$ mice and age-matched wild-type (WT) control mice. Two weeks after AAV-Cre-eGFP viral injection, we performed RNAscope *in situ* hybridization assay (Li et al., 2015) to quantify *Dtnbp1* mRNA levels in brain sections of *Dtnbp1*$^{F/F}$ and WT mice (Figure 1D). *Dtnbp1* mRNA was identified using a customized RNA probe set targeting specifically the exon 5 region of *Dtnbp1*. We found that *Dtnbp1* mRNA was substantially decreased, with only ~20% detectable *Dtnbp1* mRNA remaining in eGFP-positive cells of *Dtnbp1*$^{F/F}$ brain sections compared to that of WT control (*Dtnbp1*$^{F/F}$: $0.73 \pm 0.09\ \mu m^{-3}$, $n = 103$; WT: $4.5 \pm 0.52\ \mu m^{-3}$, $n = 85$; three mice used for each group; Kolmogorov–Smirnov test, $P < 0.0001$). We also analyzed Cre mRNA density (through Cre-specific RNA probes) in eGFP-positive cells and found no difference in brain sections of *Dtnbp1*$^{F/F}$ and WT mice (*Dtnbp1*$^{F/F}$: $3.64 \pm 0.33\ \mu m^{-3}$; WT: $3.55 \pm 0.43\ \mu m^{-3}$). Taken together, we confirmed high DTNBP1 deletion efficiency mediated by Cre recombinase both *in vitro* and *in vivo* for *Dtnbp1*$^{F/F}$ mice.

We next determined the cell-type specificity of AAV-Cre-eGFP viral expression in mouse mPFC. Since AAV-Cre-eGFP virus by itself only occupied the nucleus of infected cells with eGFP signal, we injected the mPFC of 6–8-week-old *Dtnbp1*$^{F/F}$ mice by AAV-Cre-eGFP virus together with AAV-DIO-eYFP, a virus encoding Cre-dependent eYFP (Supplementary Figures S1 and S2). The purpose of injecting this AAV viral mixture is to fill the entire cell with eYFP signal to facilitate the subsequent morphological studies. We first stained brain sections with a neuronal marker, NeuN (Figure 1E), and found that 100% eYFP-positive

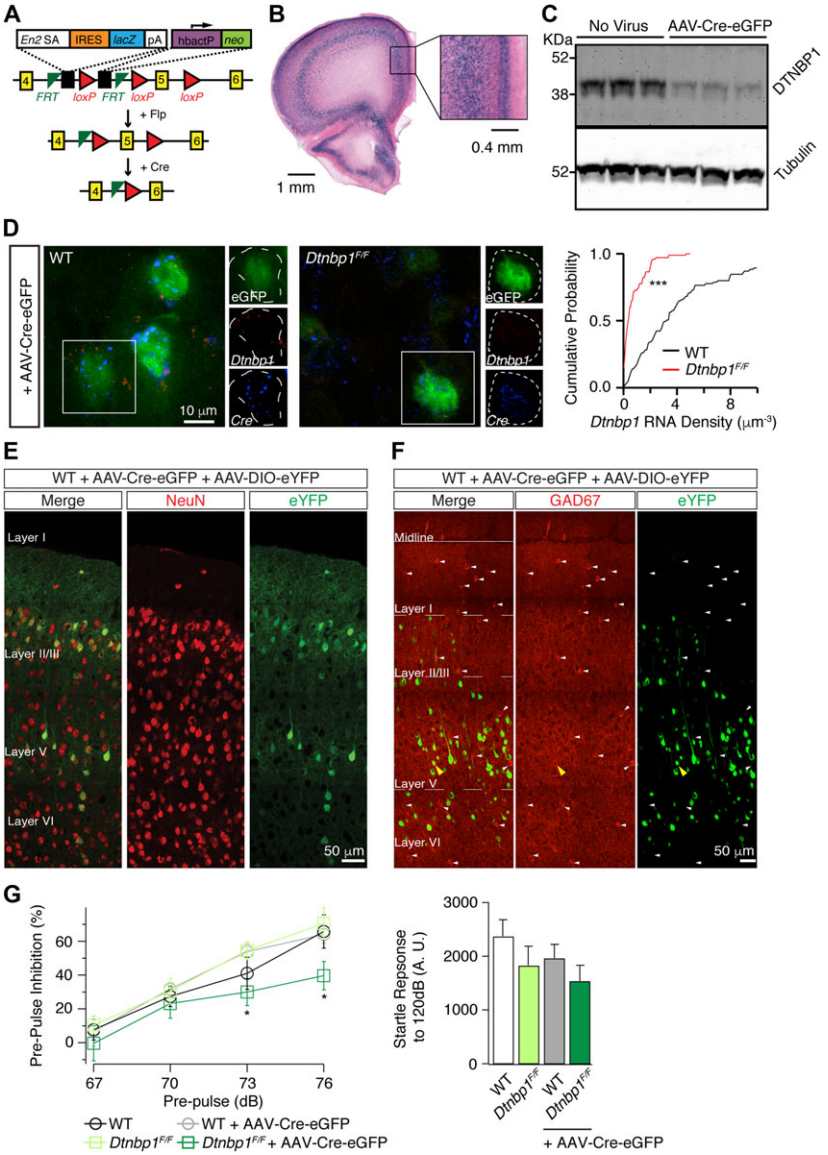

Figure 1 Deletion of DTNBP1 specifically from mPFC pyramidal neurons diminished PPI. (**A**) Schematic map for the 'knockout-first conditional-ready' *Dtnbp1* targeting cassette. Yellow numbered boxes indicated exons. Flp removed the gene-trapping *LacZ* element and converted the *Dtnbp1* allele into a true conditional allele. Cre recombinase eliminated the floxed exon 5 of *Dtnbp1*. (**B**) LacZ staining revealed the endogenous *Dtnbp1* expression pattern in adult mouse brain, obtained from the original 'knockout-first' mouse strain. (**C**) Cre-mediated deletion of DTNBP1 in cultured hippocampal neurons from $Dtnbp1^{F/F}$ embryos. Representative western blots of DTNBP1 and Tubulin from *in vitro* $Dtnbp1^{F/F}$ cultures with AAV viral infection (AAV-Cre-eGFP, 7 days post-infection) are shown. (**D**) RNAscope *in situ* hybridization assay verified *in vivo* Cre-mediated DTNBP1 deletion in mPFC of $Dtnbp1^{F/F}$ mice infected with AAV-Cre-eGFP. Left two panels were representative images showing *Dtnbp1* (red) and *Cre* (blue) mRNAs from virally infected (eGFP-positive, green) neurons of WT and $Dtnbp1^{F/F}$ mice. Dashed lines indicate infected neuronal soma. Right panel showed cumulative probability distribution of *Dtnbp1* mRNA density in eGFP-positive neurons ($Dtnbp1^{F/F}$, $n = 103$; WT, $n = 85$; three mice used for each group). (**E**) AAV-Cre-eGFP virus exclusively infected neurons in mPFC. WT mice were injected with mixed viruses of AAV-Cre-eGFP and AAV-DIO-eYFP into mPFC. Neurons were labeled with anti-NeuN antibody (red). Virally infected cells were identified with eYFP signal (green). (**F**) AAV-Cre-eGFP virus mostly infected excitatory neurons in mPFC. WT mice were injected with mixed viruses of AAV-Cre-eGFP and AAV-DIO-eYFP into mPFC. Virally infected cells were identified with eYFP (green). GABAergic neurons were identified with anti-GAD67 antibody (red) and indicated by white arrows. GAD67 and eYFP double-positive cells were marked with yellow arrowheads. (**G**) PPI in $Dtnbp1^{F/F}$ mice was reduced 14 days after AAV-Cre-eGFP injection into the mPFC. Left, PPI test for WT mice ($n = 8$), $Dtnbp1^{F/F}$ mice ($n = 10$), WT mice 2 weeks after AAV-Cre-eGFP injection (WT + AAV-Cre-eGFP, $n = 8$), and $Dtnbp1^{F/F}$ mice 2 weeks after AAV-Cre-eGFP injection ($Dtnbp1^{F/F}$ + AAV-Cre-eGFP, $n = 10$; Kolmogrov–Smirnov test, WT + AAV-Cre-eGFP vs. $Dtnbp1^{F/F}$ + AAV-Cre-eGFP: $P = 0.04$ at 73 dB, $P = 0.03$ at 76 dB). Right, startle responses to 120 dB stimuli alone. Error bars are mean ± SEM. $^{*}P < 0.05$; $^{***}P < 0.0001$.

neurons were also NeuN-positive, indicating that Cre expression was exclusively in neurons. We next stained brain sections with glutamate decarboxylase 67 (GAD67), a GABAergic neuron (inhibitory interneuron) marker (Figure 1F). And we found that only 1.1% ± 0.4% of eYFP-positive neurons were GAD67-positive, suggesting that AAV-Cre-eGFP virus (driven by CamKII promoter) predominantly (or mostly) expressed in excitatory neurons once being injected into mouse mPFC.

Dtnbp1$^{F/F}$ mice were born in a normal Mendelian ratio. Both males and females had normal weight gain and showed normal fertility. We next explored if DTNBP1 elimination specifically in excitatory neurons of mPFC would elicit any behavioral deficits. Homozygous *Dtnbp1*^{sdy} mice displayed various behavioral deficits including increased locomotion in open field, reduced social interactions, and reduced PPI of acoustic startle response (Talbot, 2009; Papaleo et al., 2012). We focally injected AAV-Cre-eGFP virus into the mPFC of 6–8-week-old *Dtnbp1*$^{F/F}$ mice and WT mice. Two weeks after viral infection, we performed various behavioral tests, including open field, social interactions, and PPI. We found that DTNBP1 deletion in excitatory neurons of mPFC did not affect either the locomotion in open field or the sociability (Supplementary Figures S3 and S4). However, we found that DTNBP1 deletion in the mPFC led to a significant reduction in PPI test without affecting the auditory reflex (Kolmogrov–Smirnov test, $P = 0.04$ at 73 dB, $P = 0.03$ at 76 dB, Figure 1G), while WT controls with the same viral injection did not display any abnormality in PPI test. Reduced PPI is a well-replicated behavior phenotype in schizophrenia patients and rodent models, indicating impaired sensorimotor gating (Swerdlow and Geyer, 1998; Braff et al., 2001; Ouagazzal and Meziane, 2012). Our observation that *Dtnbp1*$^{F/F}$ mice with DTNBP1 elimination in adult mPFC exhibited reduced PPI was consistent with previous publication that PFC was important for PPI behavior (Klamer et al., 2011; Alam et al., 2015). In addition, the fact that DTNBP1 elimination predominately in excitatory neurons of mPFC elicited a similar PPI behavioral deficit as globally DTNBP1 elimination in homozygous *Dtnbp1*^{sdy} mice (Talbot, 2009), further emphasized the importance of DTNBP1 in excitatory neurons of mPFC for maintaining prefrontal functions.

Loss of DTNBP1 in pyramidal neurons selectively impaired GABAergic transmission

To elucidate the origin of PPI behavioral deficit induced by DTNBP1 deletion in the mPFC, we analyzed synaptic activity of pyramidal neurons in acute brain slices from *Dtnbp1*$^{F/F}$ and WT mice 2 weeks after AAV-Cre-eGFP viral infection. We first recorded miniature inhibitory post synaptic currents (mIPSCs) from layer 5 pyramidal neurons in the mPFC with bath application of TTX (0.8 μM), DNQX (20 μM), and DL-AP5 (50 μM). Using eGFP fluorescent signal to identify neuron in *Dtnbp1*$^{F/F}$ mice infected with AAV-Cre-eGFP, we recorded mIPSC from pyramidal neurons expressing eGFP fluorescence signal (Cre^{+}; *Dtnbp1*-Cre) and adjacent pyramidal neurons without eGFP (Cre^{-}; *Dtnbp1*-Control). Two additional control groups were also included: layer 5 pyramidal neurons from WT mice (Naïve) and eGFP-positive neurons from WT mice injected with AAV-Cre-eGFP (Cre^{+}; WT-Cre). We found that *Dtnbp1*-Cre neurons displayed ~30% reduction in mIPSC frequency, compared with the other three control groups (Kolmogorov–Smirnov test, $P = 0.01$, *Dtnbp1*-Cre and *Dtnbp1*-Control; $P = 0.01$, Dtnbp1-Cre and WT-Cre; $P = 0.001$, *Dtnbp1*-Cre and Naïve; Figure 2A, Table 1). The amplitudes of mIPSCs were similar among the four groups (Figure 2A and Table 1). The WT-Cre neurons exhibited similar mIPSCs as Naïve neurons, indicating that viral infection itself did not affect mIPSC properties, and that the observed mIPSC frequency change in *Dtnbp1*-Cre neurons was indeed due to DTNBP1 elimination.

To examine the synaptic mechanism of GABAergic dysfunction, we recorded evoked IPSCs (eIPSCs) in brain slices from *Dtnbp1*$^{F/F}$ mice 2 weeks after AAV-Cre-eGFP infection. Stimulation electrodes were placed either laterally in layer 5 (~200 μm distance to recorded neuron) or vertically in layer 2/3 (~150 μm distance to recorded neuron), and stimuli were applied at a range of intensities. Monosynaptic IPSCs were recorded from the two groups of neurons (Cre^{+}, *Dtnbp1*-Cre; and Cre^{-}, *Dtnbp1*-Control). Both the stimulation-response curve and the maximal eIPSC responses were analyzed (Figure 2B). We found that for the maximal eIPSCs evoked at layer 5, *Dtnbp1*-Cre neurons displayed significant smaller amplitude than that of adjacent *Dtnbp1*-Control neurons (*Dtnbp1*-Cre, 2.7 ± 0.3 nA; *Dtnbp1*-Control, 1.5 ± 0.2 nA; Kolmogorov–Smirnov test, $P = 0.02$). However, stimulation at layer 2/3 elicited similar maximal eIPSCs from *Dtnbp1*-Cre (1.26 ± 0.23 nA) and adjacent *Dtnbp1*-Control neurons (1.21 ± 0.21 nA), suggesting that DTNBP1 deletion in mPFC pyramidal neurons affected perisomatic but not distal dendritic GABAergic transmissions. We also recorded paired-pulse responses at the intensity that produced half of maximal eIPSCs, and found no difference in paired-pulse ratio between *Dtnbp1*-Cre and *Dtnbp1*-Control neurons by stimulation in layer 5 or layer 2/3 (Figure 2B), indicating that presynaptic properties of GABAergic transmission were unlikely to be affected by DTNBP1 elimination.

We next determined if GABAergic synapses formed on layer 5 pyramidal neurons would be affected upon DTNBP1 elimination. To visualize the morphology of virally infected pyramidal neurons, we injected a mixture of AAV-Cre-eGFP and AAV-DIO-eYFP viruses into the mPFC of *Dtnbp1*$^{F/F}$ and WT mice. Two weeks after injection, GABAergic synapses were identified by immunostaining of vesicular GABA transporter (vGAT) on brain sections of the mPFC, and the infected neurons were identified by eYFP expression (Figure 2C). We analyzed vGAT puncta within the perisomatic region of virally infected layer 5 pyramidal neurons, and found that the density of vGAT puncta reduced by more than 20% in *Dtnbp1*$^{F/F}$ mice (0.055 ± 0.005 μm^{-2}) compared to WT controls (0.070 ± 0.003 μm^{-2}; Mann–Whitney *U*-test, $P = 0.0011$), while there was a trend but not significant increase in the sizes of puncta of *Dtnbp1*$^{F/F}$ mice (Mann–Whitney *U*-test, $P = 0.06$).

To determine whether deletion of DTNBP1 also altered excitatory transmission, we recorded miniature excitatory post synaptic currents (mEPSCs) in the presence of TTX and bicuculline (20 μM). We observed no difference in mEPSCs among the four groups (*Dtnbp1*-Cre, *Dtnbp1*-Control, WT-Cre, and Naïve)

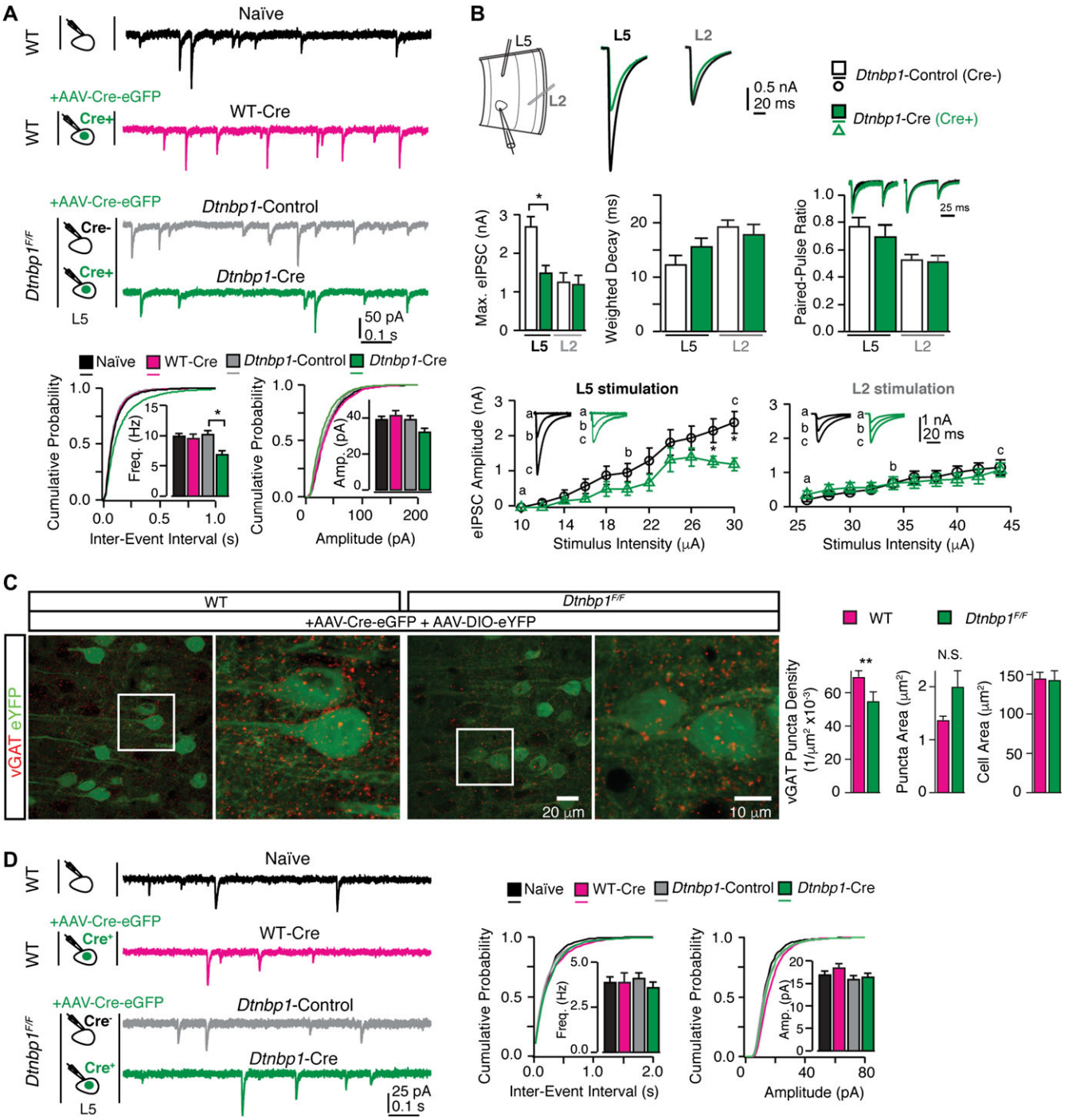

Figure 2 DTNBP1 elimination in layer 5 pyramidal neurons of mPFC specifically diminished GABAergic transmission. (**A**) Layer 5 pyramidal neurons in the mPFC of *Dtnbp1*$^{F/F}$ mice exhibited reduced mIPSC frequency upon AAV-Cre-eGFP infection (14 days), compared to their uninfected neighboring neurons. Top panel: experiment configuration and representative traces of mIPSCs. Bottom panel: cumulative distribution and quantifications (insets) of mIPSC frequency (Freq) and amplitude (Amp). Neurons from four groups were recorded and compared: neurons from WT mice without virally injection (Naïve, n = 28); virally infected neurons from WT mice (WT-Cre, n = 21); virally uninfected neurons (*Dtnbp1*-Control, n = 18), and virally infected neurons (*Dtnbp1*-Cre, n = 23) in *Dtnbp1*$^{F/F}$ mice (three mice each group, Kolmogorov–Smirnov test, P = 0.01, groups 3 and 4). (**B**) Virally infected (AAV-Cre-eGFP, 14 days) layer 5 pyramidal neurons (*Dtnbp1*-Cre) in the mPFC of *Dtnbp1*$^{F/F}$ mice exhibited diminished eIPSCs compared to their uninfected neighboring neurons (*Dtnbp1*-Control), with stimulation electrode located in layer 5 but not in layer 2/3 (n = 11 and 12 for *Dtnbp1*-Control and *Dtnbp1*-Cre with L5 stimulation, respectively; n = 13 and 17 for *Dtnbp1*-Control and *Dtnbp1*-Cre with L2 stimulation, respectively; three mice each group). Top panel (left to right): experiment paradigm;

Table 1 Quantification of mIPSC (a) and mEPSC (b) for neurons from AAV-Cre-eGFP-injected WT and *Dtnbp1*$^{F/F}$ mice.

Genotype	Group	Frequency (Hz)	Amplitude (pA)	Rise time (ms)	Decay time (ms)
(a)					
WT	Naïve	10 ± 0.4	39.1 ± 1.5	0.4 ± 0.01	5.1 ± 0.1
	Cre$^+$	9.6 ± 0.7	41.6 ± 2.4	0.4 ± 0.02	5.3 ± 0.1
Dtnbp1$^{F/F}$	Cre$^-$	10.3 ± 0.6	39.3 ± 2.0	0.4 ± 0.01	5.0 ± 0.1
	Cre$^+$	6.9 ± 0.6	32.15 ± 1.8	0.45 ± 0.01	5.9 ± 0.1
(b)					
WT	Naïve	3.9 ± 0.3	16.9 ± 0.7	0.71 ± 0.02	3.7 ± 0.1
	Cre$^+$	3.9 ± 0.5	18.5 ± 0.9	0.72 ± 0.02	3.6 ± 0.1
Dtnbp1$^{F/F}$	Cre$^-$	4.1 ± 0.3	15.9 ± 0.8	0.63 ± 0.01	3.8 ± 0.1
	Cre$^+$	3.6 ± 0.3	16.5 ± 0.7	0.65 ± 0.02	3.9 ± 0.1

(Figure 2D and Table 1). Together, these results indicate that DTNBP1 elimination in the mPFC selectively reduces the number of perisomatic GABAergic synapses on layer 5 pyramidal neurons, leading to diminished GABAergic input to these neurons.

Loss of BDNF in pyramidal neurons elicited similar GABAergic dysfunction

Interestingly, previous studies have shown similar impairments in GABAergic transmission upon gene deletion in various conditional knockout mice (Kohara et al., 2007; Bloodgood et al., 2013; Zhang et al., 2014). Among these, we were highly interested in BDNF. BDNF is secreted from postsynaptic excitatory neurons and acts locally to promote the formation of GABAergic synapse (Kohara et al., 2007). We therefore obtained heterozygous *Bdnf* conditional knockout mice (*Bdnf*$^{WT/F}$), injected AAV-Cre-eGFP into the mPFC, and recorded both mIPSCs and mEPSCs from layer 5 pyramidal neurons using the same experimental paradigm as that used for *Dtnbp1*$^{F/F}$ mice. We found that deletion of *Bdnf* in mPFC layer 5 pyramidal neurons specifically reduced the frequency of mIPSC, while mEPSCs remained unchanged (Kolmogorov–Smirnov test, $P = 0.01$ for frequency of mIPSC; Figure 3 and Table 2). The apparent similarity of GABAergic transmission deficits caused by *Dtnbp1* knockout and *Bdnf* heterozygous knockout raises an interesting possibility that DTNBP1 maintains GABAergic synapses on pyramidal neurons via BDNF.

Deletion of DTNBP1 in cultured pyramidal neurons selectively reduced GABAergic transmission

To study the potential interaction between DTNBP1 and BDNF in cultured neurons, we next examined if DTNBP1 deletion would yield similar abnormality in GABAergic transmission from cultured *Dtnbp1*$^{F/F}$ pyramidal neurons. We transfected hippocampal neurons cultured from embryonic *Dtnbp1*$^{F/F}$ mice with a plasmid encoding Cre and tdTomato separated by a self-cleaving 2A peptide (Cre-2A-tdTomato), or a control plasmid containing an inactive form of Cre (Cre^{Y324F}-2A-tdTomato). Using tdTomato signal to identify positively transfected neurons, we recorded mEPSCs and mIPSCs (recorded at −70 and 0 mV, respectively, in the presence of TTX) on the sixth day post-transfection. Consistent with our observations from *ex vivo* brain slices, DTNBP1 deletion in cultured pyramidal neurons also displayed a significant decrease in the frequency (Kolmogorov–Smirnov test, $P = 0.02$) but not in the amplitude of mIPSC, while mEPSC remained normal compared with controls (Figure 4).

DTNBP1 resides within the vicinity of BDNF molecules

DTNBP1 is a component of the biogenesis of lysosome-related organelle complex 1 (BLOC-1) (Li et al., 2003). It is important in the regulation of neurotransmitter release and receptor trafficking (Chen et al., 2008; Ji et al., 2009; Tang et al., 2009). BDNF is secreted both spontaneously and in an activity-dependent fashion from the axon, soma, and dendrites of neurons (Lessmann and Brigadski, 2009; Dean et al., 2012; Dieni et al., 2012). To determine whether DTNBP1 resided in the vicinity of BDNF-containing vesicles, we employed three-dimensional dual-color fluorescence photo-activation localization microscopy (3D-FPALM) method (Huang et al., 2008; Henriques et al., 2010) to determine the localization of DTNBP1 and BDNF in cultured pyramidal neurons from WT mice. Neurons were co-transfected with plasmids encoding BDNF-PA-mCherry

traces of averages of maximal eIPSCs recorded from layer 5 pyramidal neurons stimulated by electrodes placed in layer 5 (L5) or layer 2/3 (L2), respectively. Middle panel (left to right): averaged maximal eIPSCs quantifications (Kolmogorov–Smirnov test, $P = 0.02$, L5 stimulation); comparison of weighted-decay of maximal eIPSC of *Dtnbp1*-Cre and *Dtnbp1*-Control neurons from *Dtnbp1*$^{F/F}$ mice; paired-pulse responses for eIPSCs of *Dtnbp1*-Cre and *Dtnbp1*-Control neurons from *Dtnbp1*$^{F/F}$ mice. Traces on top showed the averaged eIPSCs from *Dtnbp1*-Control (black) and *Dtnbp1*-Cre neurons (green), normalized to the peak of the first IPSC. The paired pulses were delivered at 100 ms interval. Bottom: input–output curves of eIPSCs stimulated by a group of electrical stimuli with various intensities (Kolmogorov–Smirnov test, $P = 0.03$ for L5 stimulation). Insets, eIPSC traces at indicated stimuli. (**C**) Reduced vGAT (red) puncta density in perisomatic regions of layer 5 pyramidal neurons in *Dtnbp1*$^{F/F}$ mice compared to WT mice. Left, representative images of vGAT immunostaining with blown-up images of the regions in white squares on right side; right, bar graphs were quantifications for puncta densities, puncta sizes, and soma sizes of analyzed neurons (*Dtnbp1*$^{F/F}$, $n = 85$ neurons; WT, $n = 59$ neurons; three mice each group; Mann–Whitney *U*-test, $P = 0.0011$ for vGAT density comparison). (**D**) Deletion of DTNBP1 from mPFC pyramidal neurons did not change excitatory synaptic transmissions. Left panel: experiment configuration and representative traces of mEPSCs. Right panel: cumulative distribution and quantifications (insets) of mEPSC frequency (Freq) and amplitude (Amp). mEPSCs were recorded from virally infected neurons in *Dtnbp1*$^{F/F}$ mice (*Dtnbp1*-Cre, $n = 26$) 14 days after AAV-Cre-eGFP injection, which showed no differences compared to three other groups: neurons from WT mice without viral infection (Naïve, $n = 31$); virally infected neurons from WT mice (WT-Cre, $n = 19$); and uninfected neurons from *Dtnbp1*$^{F/F}$ mice (*Dtnbp1*-Control, $n = 26$). Error bars are mean ± SEM. *$P < 0.05$; **$P < 0.01$.

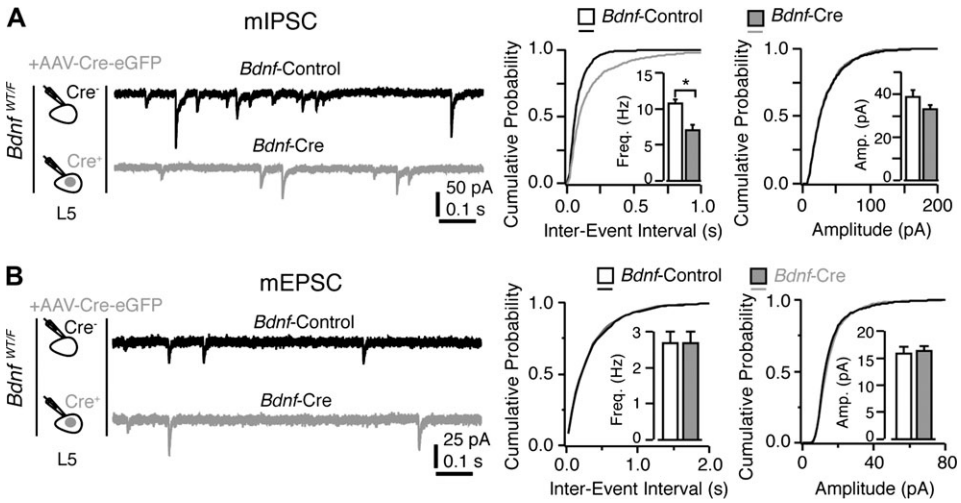

Figure 3 Deletion of BDNF in excitatory neurons of mPFC for 14 days reduced mIPSCs but not mEPSCs. (**A**) Layer 5 pyramidal neurons in the mPFC of *Bdnf*$^{WT/F}$ mice exhibited reduction in mIPSC frequency upon AAV-Cre-eGFP viral infection (14 days) compared to their uninfected neighboring neurons. Left: experiment configuration; middle: representative traces of mIPSCs; right: cumulative distribution and quantifications (insets) of mIPSC frequency (Freq, Kolmogorov–Smirnov test, $P = 0.01$) and amplitude (Amp). Two groups of neurons were compared: virally uninfected neurons in *Bdnf* $^{WT/F}$ mice (*Bdnf*-Control, $n = 24$) and virally infected neurons in *Bdnf* $^{WT/F}$ mice (*Bdnf*-Cre, $n = 20$; three mice each group). (**B**) mEPSCs recorded from virally infected neurons in *Bdnf* $^{WT/F}$ mice (*Bdnf*-Cre, $n = 24$) upon AAV-Cre-eGFP infection (14 days) showed no difference compared to adjacent uninfected neurons from *Bdnf* $^{WT/F}$ mice (*Bdnf*-Control, $n = 24$). Error bars are mean ± SEM. *$P < 0.05$.

Table 2 Quantification of mIPSC (a) and mEPSC (b) for neurons from AAV-Cre-eGFP-injected *Bdnf* $^{WT/F}$ mice.

Genotype	Group	Frequency (Hz)	Amplitude (pA)	Rise time (ms)	Decay time (ms)
(a)					
Bdnf $^{WT/F}$	Cre^-	10.8 ± 0.5	38.9 ± 2.8	0.39 ± 0.02	5.2 ± 0.1
	Cre^+	7.1 ± 0.7	33.16 ± 1.6	0.46 ± 0.01	6.2 ± 0.2
(b)					
Bdnf $^{WT/F}$	Cre^-	2.7 ± 0.3	16.0 ± 1.1	0.64 ± 0.03	3.6 ± 0.1
	Cre^+	2.7 ± 0.3	16.4 ± 0.7	0.68 ± 0.02	3.7 ± 0.2

and DTNBP1-Dronpa3. Two days after transfection, neurons were fixed. Dual-color 3D-FPALM images were acquired from somatic region of double-positive transfected pyramidal neurons, and single molecules were identified and localized for BDNF (PA-mCherry) and DTNBP1 (Dronpa3) (Figure 5A and B). We plotted the histograms of the localizations of each molecules and found that distributions of photons from each molecule follow Gaussian distribution with a full width at half maximum (FWHM) of 22 nm for BDNF with a standard deviation of 8 nm; the FWHM for DTNBP1 was 19 nm with a standard deviation of 5 nm (Figure 5C), suggesting an imaging resolution of 22 nm for dual-color 3D-FPALM imaging. We calculated the shortest distance between BDNF and DTNBP1 molecules, and analyzed the distance distribution with a Gaussian fit function: $y = k_0 + k_1\exp(-(x-k_2)^2/k_3)$. The mode of the distribution is 123.59 nm and the standard deviation is 5.18 nm (Figure 5D). Given that BDNF resides inside vesicles, whereas DTNBP1 resides in the cytosol, an average distance of DTNBP1 and BDNF being ~124 nm suggests that DTNBP1 resided in the vicinity of BDNF-containing vesicles.

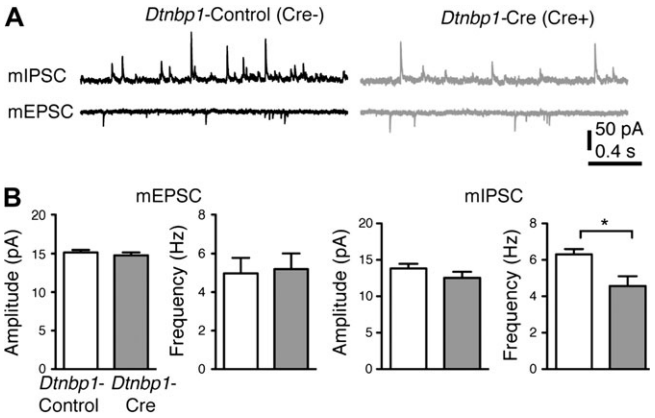

Figure 4 Deletion of DTNBP1 in cultured hippocampal neurons from *Dtnbp1*$^{F/F}$ mice specifically diminished the inhibitory synaptic transmission. (**A**) Representative traces of mIPSCs and mEPSCs recorded from uninfected control (*Dtnbp1*-Control, $n = 23$) and virally infected neurons (*Dtnbp1*-Cre, $n = 24$) of *in vitro* cultured hippocampal neurons from *Dtnbp1*$^{F/F}$ mice. (**B**) Quantifications of amplitude and frequency of mEPSCs (left) and mIPSCs (right; Kolmogorov–Smirnov test, $P = 0.02$ for frequency comparison). Error bars are mean ± SEM. *$P < 0.05$.

Deletion of DTNBP1 specifically reduced activity-dependent BDNF release

BDNF exerts its function by being secreted into extracellular space and subsequently binding to its receptors to activate downstream signaling pathways. To examine how DTNBP1 elimination would affect BDNF function, we monitored BDNF

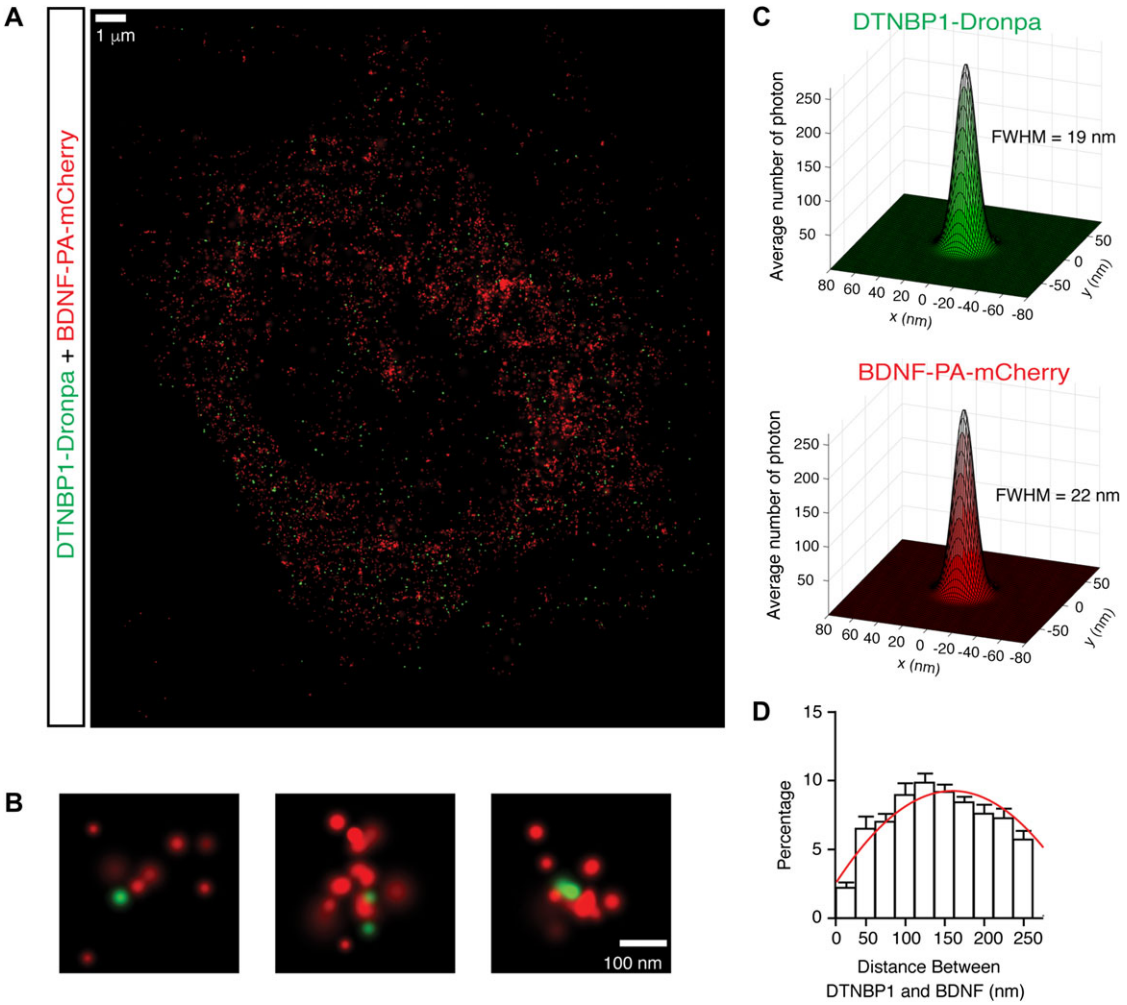

Figure 5 DTNBP1 resides in the vicinity of BDNF. (**A**) Representative image of BDNF and DTNBP1 localization in cultured hippocampal neuron. (**B**) Representative images of co-localization of BDNF (tagged with PA-mCherry, red) and DTNBP1 (tagged with Dronpa, green) revealed through 3D-FPALM super-resolution microscopy. (**C**) The localization distributions of the BDNF and DTNBP1 clusters. Histograms of localizations were generated by aligning center of mass. The histograms were fitted to a Gaussian function to determine FWHM. (**D**) Distribution of minimal distances between BDNF and DTNBP1 molecules (n = 17 neurons), fitted with Gaussian distribution (red line). Error bars are mean ± SEM.

secretion in cultured pyramidal neurons. We generated a plasmid encoding pHluorin tagged BDNF (BDNF-pH) and employed total internal reflection fluorescence (TIRF) microscopy to visualize BDNF secretion (Lin et al., 2009; Li et al., 2012a, b; Daly et al., 2015). We co-transfected cultured *Dtnbp1*$^{F/F}$ neurons with the plasmid mixture of BDNF-pH and Cre-2A-tdTomato, or BDNF-pH and Cre^{Y324F}-2A-tdTomato as control. Six days after transfection, we recorded spontaneous BDNF secretion events in the presence of TTX, or activity-dependent BDNF secretion elicited by bath application of 50 mM KCl (Figure 6). We found that neurons with DTNBP1 deletion (i.e. Cre transfected neurons) displayed a trend but not significant reduction in spontaneous BDNF secretion (Mann–Whitney *U*-test, P = 0.17, Figure 6A). However, neurons with DTNBP1 deletion exhibited ~50% reduction in the frequency of activity-dependent BDNF secretion, compared to the Cre^{Y324F} transfected control neurons (Mann–Whitney *U*-test, P = 0.0002, Figure 6B). We also compared BDNF activity-dependent secretion in WT neurons transfected with Cre and Cre^{Y324F}, and found no difference between these two groups (Figure 6C). These results suggest that DTNBP1 facilitates activity-dependent BDNF secretion in pyramidal neurons.

BDNF overexpression did not rescue GABAergic deficit after DTNBP1 deletion

We hypothesized that DTNBP1 elimination in pyramidal neurons results in BDNF release deficiency, consequently leading to diminished GABAergic synapses on pyramidal neurons. To test this hypothesis, we first virally overexpressed BDNF in pyramidal neurons from *Dtnbp1*$^{F/F}$ mice to determine if increasing of BDNF expression could rescue impaired GABAergic transmission upon DTNBP1 deletion. We generated an AAV viral construct with CaMKII promoter to express tdTomato and BDNF separated

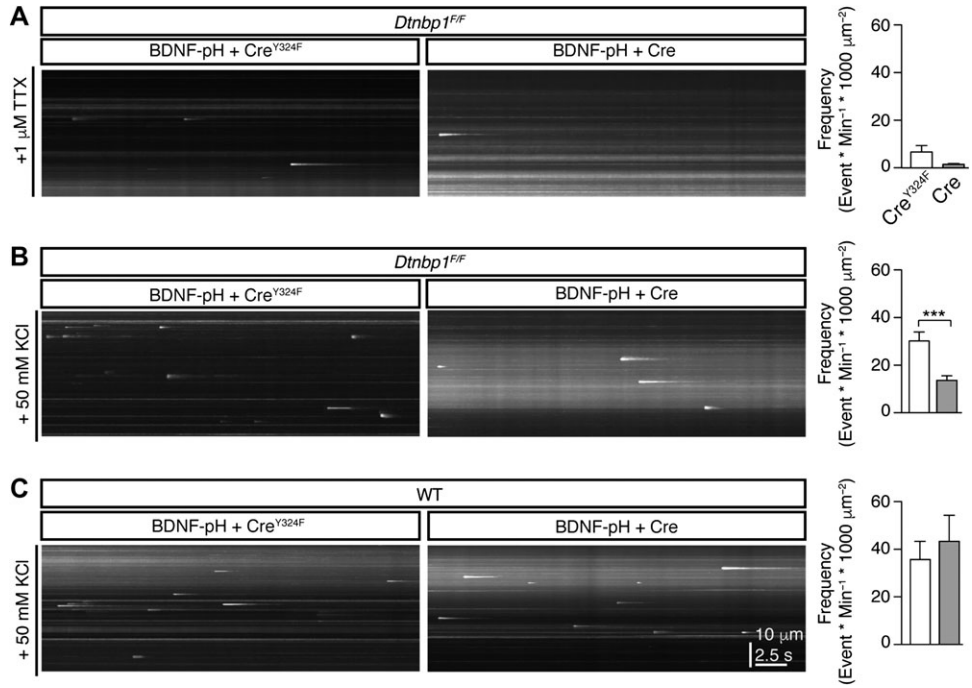

Figure 6 DTNBP1 facilitated activity-dependent BDNF secretion. (**A**) Deletion of DTNBP1 did not change spontaneous BDNF secretion in cultured *Dtnbp1*$^{F/F}$ hippocampal neurons. Bath application of TTX was used to block firing of neurons. Left: representative *y-t* maximal intensity projection of TIRF images for BDNF-pH secretion. Right: quantifications of BDNF release events (Cre^{Y324F}, n = 89; Cre, n = 84; Mann–Whitney *U*-test, P = 0.17). (**B**) Deletion of DTNBP1 reduced activity-dependent BDNF secretion in cultured *Dtnbp1*$^{F/F}$ hippocampal neurons. Bath application of 50 mM KCl was used to stimulate activity-dependent BDNF secretion. Left: representative *y-t* maximal intensity projection of TIRF images for BDNF-pH secretion. Right: quantifications of BDNF release events (Cre^{Y324F}, n = 45; Cre, n = 46; Mann–Whitney *U*-test, P = 0.0002). (**C**) Plasmid infection of Cre or Cre^{Y324F} did not change activity-dependent BDNF secretion in WT cultured hippocampal neurons. Bath application of 50 mM KCl was used to stimulate activity-dependent BDNF secretion. Left: representative *y-t* maximal intensity projection of TIRF images for BDNF-pH secretion. Right: quantifications of BDNF release events (Cre^{Y324F}, n = 24; Cre, n = 25). Error bars are mean ± SEM. ***$P < 0.001$.

by a self-cleaving 2 A peptide (AAV-tdTomato-2A-BDNF). We co-injected AAV-tdTomato-2A-BDNF and AAV-Cre-eGFP into mPFC of *Dtnbp1*$^{F/F}$ and *Bdnf*$^{WT/F}$ mice. We then recorded mIPSCs from acute brain slices 2 weeks after viral injection. On these brain slices, we identified three groups of layer 5 pyramidal neurons in the mPFC: (i) neurons with no fluorescence expression (Control); (ii) neurons expressing eGFP in nucleus only (Cre); and (iii) neurons expressing both tdTomato in cytosol and eGFP in nucleus (Cre-BDNF). Our recordings from *Bdnf*$^{WT/F}$ mice showed that Cre neurons still exhibited a reduced mIPSC frequency compared to Control neurons, while the Cre-BDNF neurons displayed a normal mIPSC frequency (Kolmogorov–Smirnov test, P = 0.007 for comparison between Control and Cre; P = 0.003 for comparison between Cre and Cre-BDNF, Figure 7A and Table 3). These results demonstrate that virally expressed BDNF was able to rescue endogenous deficiency of BDNF in those mice. However, Cre-BDNF neurons in *Dtnbp1*$^{F/F}$ mice still exhibited reduced mIPSC frequency compared to Control neurons, similar to that of Cre neurons (Kolmogorov–Smirnov test, P = 0.01 for comparison between Control and Cre; P = 0.04 for comparison between Control and Cre-BDNF, Figure 7B and Table 3). These results suggest that in the absence of DTNBP1, virally expressed BDNF is not efficiently secreted, and therefore is not able to rescue the impairments caused by *Dtnbp1* deletion.

BDNF infusion into mPFC rescued synaptic and behavior deficits after DTNBP1 deletion

We next asked whether restoration of extracellular BDNF level through BDNF infusion into the mPFC would rescue the deficits elicited by DTNBP1 elimination. Immediately after AAV-Cre-eGFP virus injection in *Dtnbp1*$^{F/F}$ mice, a cannula connected with osmotic pump containing 20 μg/ml BDNF in ACSF was implanted into the mPFC (Nagahara et al., 2009). Through this cannula, osmotic pump constantly delivered exogenous BDNF into the mPFC for 2 weeks. In control *Dtnbp1*$^{F/F}$ and WT mice, a cannula connected with osmotic pump containing only ACSF was implanted after AAV-Cre-eGFP virus injection. A total of four groups of layer 5 pyramidal neurons were recorded and compared: (i) AAV-Cre-eGFP-infected neurons from WT mice with ACSF infusion (WT-Cre + ACSF); (ii) AAV-Cre-eGFP-infected neurons from *Dtnbp1*$^{F/F}$ mice with ACSF infusion (*Dtnbp1*-Cre + ACSF); (iii) uninfected neurons from *Dtnbp1*$^{F/F}$ mice with BDNF infusion (*Dtnbp1*-Control + BDNF); and (iv) AAV-Cre-eGFP-infected neurons from *Dtnbp1*$^{F/F}$ mice with BDNF infusion (*Dtnbp1*-Cre + BDNF).

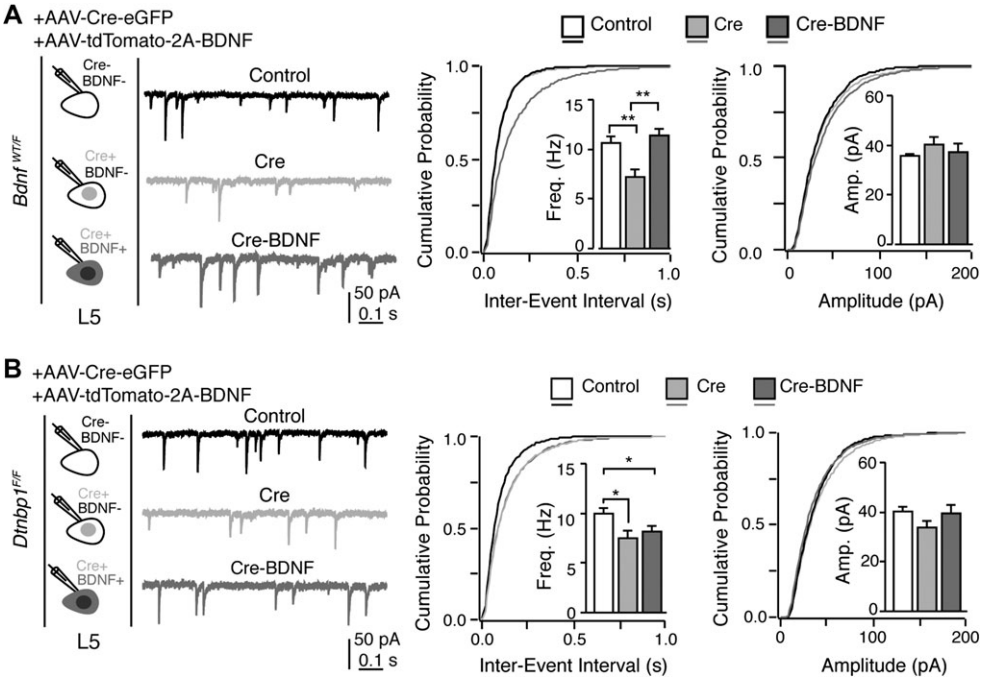

Figure 7 Viral expression of BDNF failed to restore the abnormal inhibitory transmission induced by DTNBP1 deletion. (**A**) Viral expression of BDNF sufficiently restored the abnormalities in inhibitory transmission induced by BDNF deletion in *Bdnf*$^{WT/F}$ mice. Left: experiment configuration and representative traces of mIPSCs. Right: cumulative distribution and quantifications (insets) of mIPSC frequency (Freq) and amplitude (Amp). Three groups of neurons were recorded and compared in *Bdnf* $^{WT/F}$ mice: uninfected neurons (Control, n = 17 from three mice); AAV-Cre-eGFP-infected neurons (Cre, n = 19 from three mice); AAV-Cre-eGFP and AAV-tdTomato-2A-BDNF co-infected neurons (Cre-BDNF, n = 16 from three mice). Kolmogorov–Smirnov test, P = 0.007 comparing Control to Cre; P = 0.003 comparing Cre and Cre-BDNF. (**B**) Viral expression of BDNF failed to restore the abnormal inhibitory transmission induced by DTNBP1 deletion in *Dtnbp1*$^{F/F}$ mice. Three groups of neurons were recorded and compared in *Dtnbp1*$^{F/F}$ mice: uninfected neurons (Control, n = 19 from three mice); AAV-Cre-eGFP-infected neurons (Cre, n = 18 from three mice); AAV-Cre-eGFP and AAV-tdTomato-2A-BDNF co-infected neurons (Cre-BDNF, n = 22 from three mice). For the mIPSC frequency comparison, Kolmogorov–Smirnov test, P = 0.01 comparing Control to Cre; P = 0.04 comparing Control to Cre-BDNF. Error bars are mean ± SEM. *P < 0.05; **P < 0.01.

We found that BDNF infusion into the mPFC rescued dysfunctional GABAergic transmission in pyramidal neurons with DTNBP1 deletion, as '*Dtnbp1*-Cre + BDNF' neurons and adjacent '*Dtnbp1*-Control + BDNF' neurons displayed similar mIPSC frequency in *Dtnbp1*$^{F/F}$ mice with BDNF infusion (Figure 8A and Table 4). This rescue effect is not due to surgery or chronic infusion, as '*Dtnbp1*-Cre + ACSF' neurons in *Dtnbp1*$^{F/F}$ mice infused with ACSF still exhibited decreased mISPC frequency compared to the control 'WT-Cre + ACSF' neurons in WT mice infused with ACSF (Kolmogorov–Smirnov test, P = 0.03, 'WT-Cre + ACSF' to '*Dtnbp1*-Cre + ACSF', Figure 8A and Table 4). Following BDNF perfusion, the amplitude of mIPSC in '*Dtnbp1*-Cre + BDNF' also increased, which might reflect homeostatic response after chronic loss of BDNF in these neurons. These results suggest that extracellular BDNF is important for maintaining GABAergic transmission to pyramidal neurons in the mPFC.

We next examined if BDNF infusion in the mPFC could restore the loss of perisomatic GABAergic synapses induced by DTNBP1 deletion. We injected a viral mixture of AAV-Cre-eGFP and AAV-DIO-eYFP into the mPFC of *Dtnbp1*$^{F/F}$ mice. We then focally infused ACSF or BDNF through osmotic pump. Two weeks later, we obtained brain sections for vGAT immunostaining. WT mice injected with viral mixture and infused with ACSF served as additional control. EYFP signals were used to outline the virally infected layer 5 pyramidal neurons, and vGAT puncta were analyzed within the perisomatic regions of infected neurons in the three groups of mice (WT + ACSF, *Dtnbp1*$^{F/F}$ + ACSF, *Dtnbp1*$^{F/F}$ + BDNF; Figure 8B). We found that BDNF infusion in *Dtnbp1*$^{F/F}$ mice fully restored GABAergic

Table 3 Quantification of mIPSCs for neurons from AAV-Cre-eGFP and AAV-tdTomato-2A-BDNF co-injected *Bdnf* $^{WT/F}$ mice (a) and *Dtnbp1*$^{F/F}$ mice (b).

Genotype	Group	Frequency (Hz)	Amplitude (pA)	Rise time (ms)	Decay time (ms)
(a)					
Bdnf $^{WT/F}$	Cre$^-$ BDNF$^-$	10.7 ± 0.6	35.9 ± 0.4	0.24 ± 0.02	5.4 ± 0.4
	Cre$^+$ BDNF$^-$	7.3 ± 0.7	40.8 ± 2.5	0.14 ± 0.02	5.3 ± 0.5
	Cre$^+$ BDNF$^+$	11.5 ± 0.6	37.7 ± 3.0	0.14 ± 0.02	5.2 ± 0.5
(b)					
Dtnbp1$^{F/F}$	Cre$^-$ BDNF$^-$	10.1 ± 0.5	40.6 ± 1.6	0.38 ± 0.01	5.0 ± 0.2
	Cre$^+$ BDNF$^-$	7.6 ± 0.7	34.1 ± 2.2	0.45 ± 0.01	5.6 ± 0.2
	Cre$^+$ BDNF$^+$	8.3 ± 0.5	40.0 ± 3.0	0.45 ± 0.01	5.2 ± 0.1

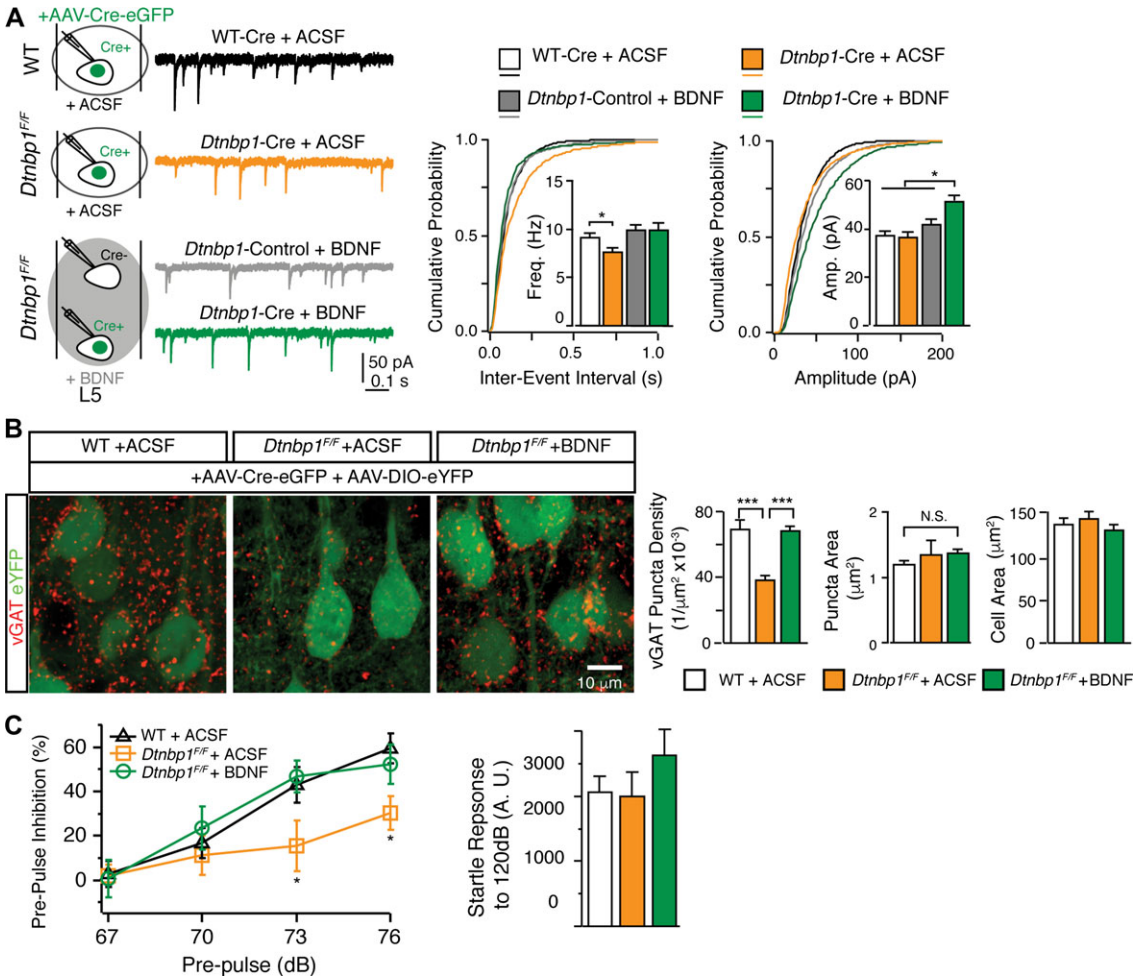

Figure 8 Extracellular infusion of BDNF restored functional deficits induced by DTNBP1 deletion in mPFC. (**A**) Application of BDNF via intracerebral infusion (14 days) efficiently restored the diminished mIPSC frequency induced by DTNBP1 deletion in *Dtnbp1*$^{F/F}$ mice. Left: experiment configuration and representative traces of mIPSCs. Right: cumulative distributions and quantifications (insets) of mIPSC frequency (Freq) and amplitude (Amp). Four groups of neurons were recorded and compared: AAV-Cre-eGFP-infected neurons from WT mice infused with ACSF (WT-Cre + ACSF, n = 18 from three mice); AAV-Cre-eGFP-infected neurons from *Dtnbp1*$^{F/F}$ mice infused with ACSF (*Dtnbp1*-Cre + ACSF, n = 22 from three mice); uninfected neurons from *Dtnbp1*$^{F/F}$ mice infused with BDNF (*Dtnbp1*-Control + BDNF, n = 16 from three mice); and AAV-Cre-eGFP-infected neurons from *Dtnbp1*$^{F/F}$ mice infused with BDNF (*Dtnbp1*-Cre + BDNF, n = 25 from three mice). For the mIPSC frequency comparison, Kolmogorov–Smirnov test, P = 0.03 comparing 'WT-Cre + ACSF' to '*Dtnbp1*-Cre + ACSF'. For the mIPSC amplitude comparison, Kolmogorov–Smirnov test, P = 0.001, 0.04, or 0.04 comparing '*Dtnbp1*-Cre + BDNF' to 'WT-Cre + ACSF', '*Dtnbp1*-Cre + ACSF', or '*Dtnbp1*-Control + BDNF', respectively. (**B**) Extracellular application of BDNF via intracerebral infusion in *Dtnbp1*$^{F/F}$ mice efficiently restored GABAergic synapse densities to control levels. Cre-expressing neurons were identified with eYFP signal (green). Left: representative images of vGAT puncta (red) (scale bar, 10 μm); right: quantifications of vGAT puncta densities, puncta sizes, and soma sizes for analyzed neurons. Neurons from three groups of mice were compared: WT mice with ACSF infusion (1. WT + ACSF, n = 108, three mice); *Dtnbp1*$^{F/F}$ mice with ACSF infusion (2. *Dtnbp1*$^{F/F}$ + ACSF, n = 82, two mice); *Dtnbp1*$^{F/F}$ mice with BDNF infusion (3. *Dtnbp1*$^{F/F}$ + BDNF, n = 138, three mice; Mann–Whitney U-test, $P < 0.0001$, group 1 vs. group 2; $P < 0.0001$, group 2 vs. group 3). (**C**) Extracellular application of BDNF via intracerebral infusion efficiently restored deficit in PPI test induced by DTNBP1 deletion in *Dtnbp1*$^{F/F}$ mice. Left: PPI test for WT mice infused with ACSF (1. WT + ACSF), *Dtnbp1*$^{F/F}$ mice infused with ACSF (2. *Dtnbp1*$^{F/F}$ + ACSF), and *Dtnbp1*$^{F/F}$ mice infused with BDNF (3. *Dtnbp1*$^{F/F}$ + BDNF) (n = 8 mice each group; Kolmogorov–Smirnov test; P = 0.002, group 1 vs. group 2 at 73 dB; P = 0.03, group 2 vs. group 3 at 73 dB; P = 0.02, group 1 vs. group 2 at 76 dB; P = 0.03, group 2 vs. group 3 at 76 dB). Right: startle responses to 120 dB stimuli for all tested mice. Error bars are mean ± SEM. *$P < 0.05$; ***$P < 0.001$.

synapse density in the perisomatic region of Cre-expressing neurons, while Cre-positive neurons from ACSF infused *Dtnbp1*$^{F/F}$ mice still showed a loss of GABAergic synapse (WT + ACSF, 0.069 ± 0.005 μm^{-2}; *Dtnbp1*$^{F/F}$ + ACSF, 0.039 ± 0.002 μm^{-2}; *Dtnbp1*$^{F/F}$ + BDNF, 0.068 ± 0.003 μm^{-2}; Mann–Whitney U-test, $P < 0.0001$, WT + ACSF to *Dtnbp1*$^{F/F}$ + ACSF; $P < 0.0001$, *Dtnbp1*$^{F/F}$ + ACSF to *Dtnbp1*$^{F/F}$ + BDNF). We did not observe any difference in puncta size among the three groups.

Table 4 Quantification of mIPSCs for neurons from extracellular application of BDNF in AAV-Cre-eGFP-injected *Dtnbp1*$^{F/F}$ mice.

Genotype and treatment	Group	Frequency (Hz)	Amplitude (pA)	Rise time (ms)	Decay time (ms)
WT + ACSF	Cre^{+}	9.2 ± 0.4	37.7 ± 1.6	0.38 ± 0.01	4.5 ± 0.1
Dtnbp1$^{F/F}$ +ACSF	Cre^{+}	7.7 ± 0.4	37.0 ± 2.0	0.47 ± 0.02	5.9 ± 0.2
Dtnbp1$^{F/F}$ +BDNF	Cre^{-}	10.0 ± 0.5	42.3 ± 1.9	0.42 ± 0.02	4.9 ± 0.1
	Cre^{+}	10.2 ± 0.7	51.6 ± 2.2	0.39 ± 0.01	4.8 ± 0.1

Finally, we investigated if BDNF infusion into the mPFC could rescue PPI behavioral deficit observed after DTNBP1 deletion. *Dtnbp1*$^{F/F}$ and WT mice were injected with AAV-Cre-eGFP and implanted with osmotic pumps to focally infuse BDNF or ACSF into the mPFC. Two weeks later PPI responses were tested on these mice (Figure 8C). We found that BDNF infusion completely rescued behavioral deficits in *Dtnbp1*$^{F/F}$ mice injected with AAV-Cre-eGFP, as these mice displayed normal PPI responses comparable to those of WT mice. However, *Dtnbp1*$^{F/F}$ mice injected with AAV-Cre-eGFP and infused with ACSF still showed deficits in PPI response, at a similar level to what we originally observed in *Dtnbp1*$^{F/F}$ mice injected with AAV-Cre-eGFP (Kolmogorov–Smirnov test; $P = 0.002$, WT + ACSF to *Dtnbp1*$^{F/F}$ + ACSF at 73 dB; $P = 0.03$, *Dtnbp1*$^{F/F}$ + ACSF to *Dtnbp1*$^{F/F}$ + BDNF at 73 dB; $P = 0.02$, WT + ACSF to *Dtnbp1*$^{F/F}$ + ACSF at 76 dB; $P = 0.03$, *Dtnbp1*$^{F/F}$ + ACSF to *Dtnbp1*$^{F/F}$ + BDNF at 76 dB). No difference in startle responses to 120 dB stimuli was observed among these mice. Together, these results strongly support our hypothesis that DTNBP1 facilitates BDNF secretion to maintain prefrontal function.

Discussion

In this study, we showed that DTNBP1 played a key role in the regulation of GABAergic transmission in the mPFC. Deletion of *Dtnbp1* in pyramidal neurons of the mPFC led to reduction in perisomatic GABAergic synapses and deficit in PPI behavior. Using advanced microscopy methods, we further demonstrated that DTNBP1 regulated activity-dependent BDNF secretion. Finally, we showed that increasing extracellular BDNF level in the mPFC restored inhibitory transmission and behavioral deficit elicited by DTNBP1 elimination.

Most schizophrenia patients are not carriers of *Dtnbp1* mutations, but still exhibit lower expression levels of DTNBP1 in specific brain regions (Talbot et al., 2004; Weickert et al., 2008). Previous studies have shown that global deletion of DTNBP1 in *Dtnbp1*^{sdy} mice leads to dysfunction of multiple neuronal circuits (Li et al., 2003; Chen et al., 2008; Ji et al., 2009; Tang et al., 2009; Carlson et al., 2011). In the present study, we use a conditional *Dtnbp1* knockout mouse model to illustrate cell type-specific functions of DTNBP1, and in particular, how deficiency of this molecule may contribute to schizophrenia pathology.

We demonstrated that DTNBP1 elimination specifically from pyramidal neurons in the mPFC elicited reduced PPI. PPI is the phenomenon in which a weak pre-stimulus (pre-pulse) suppresses the response to a following startling stimulus. PPI is observed cross-species, highly conserved among vertebrates and tested in a similar fashion in both human and rodents. Impaired PPI was often observed in schizophrenia patients (Braff et al., 2001) and several other neuropsychiatric disorders, including Huntington's disease (Swerdlow et al., 1995), obsessive-compulsive disorder (Swerdlow et al., 1993), bipolar patients (Perry et al., 2001), Tourette's syndrome (Swerdlow et al., 2001b), and autism patients (Perry et al., 2007). Many mouse genetic models of schizophrenia, including *Dtnbp1*^{sdy} mice, also showed deficits in PPI (Powell et al., 2009; Talbot, 2009; Papaleo et al., 2012). PPI impairment is thought to reflect deficits in an inhibition mechanism for sensorimotor gating, and a variety of brain regions were identified to be involved in brain circuitry regulating PPI, such as mPFC, hippocampus, and striatum (Swerdlow et al., 2001a). Pharmacological studies have revealed that lesion and disruption of neuronal activity in the PFC impaired PPI (Swerdlow et al., 2008). Reports also showed that manipulation of inhibitory transmission by modulating $GABA_A$ receptors in the mPFC compromised cognitive function and PPI (Japha and Koch, 1999; Pezze et al., 2014). Our observation suggests that DTNBP1 deficiency in adult mPFC is a risk factor for PPI impairment. It is worth to point out here that since only male mice were used in our experiments, future studies should examine whether the same findings hold true for female mice.

The role of inhibitory transmission in mPFC is well documented and dysfunction of inhibitory circuitry in the mPFC is now recognized as a prominent clinical feature of schizophrenia (Lewis et al., 2005; Lewis, 2014). Post-mortem analysis from schizophrenic patients revealed a significant loss of GABAergic axon terminals (Woo et al., 1998) and prominent low expression level of *GAD67*, an essential enzyme of GABA neurotransmitter synthesis (Hashimoto et al., 2003). Previous studies from *Dtnbp1*^{sdy} mice also suggested an association between DTNBP1 deficiency and the impaired GABAergic signaling, including reduced activity of fast-spiking (FS) interneurons (Ji et al., 2009), reduced parvalbumin immunoreactivity, and abnormal gamma-band oscillations in cortical network (Carlson et al., 2011).

Here, using a *Dtnbp1* conditional knockout mouse strain, we revealed a cell type-specific mechanism of DTNBP1 in regulating GABAergic signaling. We demonstrated that deletion of DTNBP1 specifically from pyramidal neurons of adult mPFC elicited dysfunctional GABAergic transmission. Our electrophysiological recordings demonstrated a significant reduction in the frequency of mIPSC but not that of mEPSC in pyramidal neurons with DTNBP1 deletion. Immunostainings of vGAT puncta further showed the loss of GABAergic synapses in the perisomatic region of pyramidal neurons upon DTNBP1 deletion. These observations suggest that DTNBP1 is important for the maintenance of GABAergic synapses on pyramidal neurons.

Our electrophysiology study using *Dtnbp1*$^{F/F}$ mice injected with AAV-Cre-eGFP (driven by CaMKII promoter) showed that cortical pyramidal neurons with DTNBP1 deletion (i.e. Cre-positive neurons) exhibited impaired IPSCs, while their adjacent Cre-negative excitatory neurons showed normal IPSCs comparable to those of WT mice.

Notably, this observation is similar to a previous report that complete loss of endogenous BDNF elicited local reduction of GABAergic synapses on pyramidal neurons (Kohara et al., 2007). We further showed that Cre virally infected cortical pyramidal neurons from heterozygous $Bdnf^{WT/F}$ mice displayed a similar impairment in IPSCs as in those of $Dtnbp1^{F/F}$ mice. We chose to study heterozygous $Bdnf^{WT/F}$ instead of homozygous $Bdnf^{F/F}$ mice, based on our results from *in vitro* TIRFM experiment, in which DTNBP1 deletion in pyramidal neurons did not completely abolished BDNF secretion, instead reduced activity-dependent BDNF secretion by ~50%. Homozygous $Bdnf^{F/F}$ mice were previously characterized to exhibit an almost complete loss of BDNF expression upon Cre exposure (Rios et al., 2001). Therefore, we assumed that $Bdnf^{WT/F}$ mice and $Dtnbp1^{F/F}$ mice would display similar level of BDNF upon Cre exposure.

Interestingly, our results suggested that DTNBP1 deletion in pyramidal neurons reduced GABAergic transmission preferentially at perisomatic region. A similar finding was also observed on CA1 pyramidal neurons in $Bdnf^{F/F}$ mice (Bloodgood et al., 2013). In this study, eIPSCs from BDNF deleted neurons were significantly smaller with stimulation at stratum pyramidale, but not at stratum radiatum or stratum oriens. These observations suggest that BDNF is essential for perisomatic GABAergic synapses. It is well known that perisomatic GABAergic synapses on pyramidal neurons mainly from FS parvalbumin-positive neurons. A previous study showed that BDNF is critical for FS neurons to establish inhibitory circuitry (Berghuis et al., 2004). Further studies are needed to determine whether BDNF secretion is also important for the development and maintenance of GABAergic synapses formed with other types of interneurons. Our results, together with evidence in the literature, strongly support the notion that BDNF plays a key role in the maintenance of GABAergic synapses on excitatory neurons, and that DTNBP1 regulates GABAergic transmission on excitatory neurons via BDNF.

BDNF is a secreted protein. Extensive studies have demonstrated that BDNF regulates synaptic activities and is involved in many important processes in neural circuit development and function, such as neuronal survival, differentiation, synapse formation and maturation (Park and Poo, 2013). Based on results from our *in vitro* TIRFM study, we propose that DTNBP1 maintains GABAergic synapses through facilitating activity-dependent BDNF secretion. We are aware of the alternative possibility that DTNBP1 affect activity-dependent BDNF transcription rather than trafficking. A recent study demonstrated that deletion of NPAS4 in hippocampal CA1 pyramidal neurons impaired their inhibitory inputs, in part through NPAS4-dependent regulation of BDNF transcription (Bloodgood et al., 2013). However, in our *in vitro* TIRFM study system, the BDNF-pHluorin plasmid did not include the activity-dependent promoter of BDNF. Instead, the pHluorin tagged pro-BDNF expression was under the control of regular CAG promoter. Since our plasmid encoding BDNF does not contain the activity-dependent BDNF promoter, our observation that DTNBP1 elimination led to diminished BDNF secretion does not support a role for DTNBP1 in regulating activity-dependent BNDF transcription. It has been shown that BDNF is stored in large dense-core vesicles (LDCV) before secretion in hippocampal pyramidal neurons (Xia et al., 2009; Dieni et al., 2012). LDCVs mediate release of neuropeptides from neurons and endocrine cells, and the size of these vesicles varies 100–200 nm (Bruns et al., 2000; Klyachko and Jackson, 2002; Chen et al., 2008; Zhang et al., 2011). Using the 3D-FPALM super-resolution microscopy method, we found that the distance between BDNF and DTNBP1 molecules falls within this range, indicating DTNBP1 could bind to BDNF-containing vesicle.

DTNBP1 could regulate transport, sorting, trafficking and secretion of LDCV, as a subunit of the endosomal sorting complex BLOC-1. A recent study suggested that LDCV secretion was regulated by DTNBP1, and that intracellular dialysis of DTNBP1 fully restored this process in $Dtnbp1^{sdy}$ mice (Chen et al., 2008). In the present study, we showed that DTNBP1 deletion in pyramidal neurons diminished preferentially activity-dependent BDNF secretion. It was previously shown that DTNBP1 deletion disrupted intracellular calcium signaling, and decreased expression of several proteins involved in synaptic vesicle priming (Saggu et al., 2013). Therefore, it is more likely that DTNBP1 facilitate activity-dependent BDNF secretion through its involvement in endosomal sorting and/or intracellular calcium signaling. Further studies are needed to unravel the underlying molecular mechanism by which DTNBP1 regulates activity-dependent BDNF secretion.

Both *DTNBP1* and *BDNF* have been associated with schizophrenia (Straub et al., 2002; Szekeres et al., 2003; Gratacos et al., 2007), and decreased expression of DTNBP1 in brain and decreased serum BDNF concentration have been reported in schizophrenic patients (Weickert et al., 2003; Green et al., 2011; Martinotti et al., 2012). Here, we offer *in vivo* evidence strongly supporting a unique connection between these two psychiatric risk factors.

A recent publication from Yuan et al. (2015) reported that DTNBP1 knockdown using shRNAs in cultured rat cortical neurons reduced BDNF exocytosis and GABAergic synapses formed on those neurons *in vitro*. This finding suggests that DTNBP1 regulates BDNF secretion. Yuan et al. (2015) also showed that exogenous BDNF application in the culture medium restored the GABAergic dysfunction associated with DTNBP1 deletion by shRNAs. In comparison, we showed that *in vivo* DTNBP1 deletion led to specific loss of perisomatic GABAergic synapses on pyramidal neurons of mouse mPFC, and led to impaired PPI behavioral response. Importantly, we performed BDNF rescue experiment *in vivo*, and demonstrated that dysfunctional GABAergic transmission and behavioral deficits induced by loss of DTNBP1 were fully restored with chronic BDNF infusion into the mPFC.

In sum, in the present study we demonstrated the cell type-specific function of DTNBP1 in pyramidal neurons. DTNBP1 maintains perisomatic GABAergic synapses on pyramidal neurons through facilitating activity-dependent BDNF secretion. Excitatory neuron-specific deletion of *Dtnbp1* in the mPFC reduced GABAergic

neurotransmission and disrupted PPI behavior. Extracellular application of BDNF into the mPFC rescued abnormalities in both GABAergic transmission and PPI behavior. The success of *in vivo* BDNF rescue experiment highlights restoration of extracellular BDNF as a potential therapeutic strategy for schizophrenia.

Materials and methods

All experiments were conducted at the National Institute on Drug Abuse Intramural Research Program in accordance with the Institutional Animal Care and Use Committee of the National Institutes of Health guidelines. Male mice were used across the studies.

For detailed methods, please see the Supplementary Materials and methods.

Supplementary material

Supplementary material is available at *Journal of Molecular Cell Biology* online.

Funding

This work is supported by the Intramural Research Program of National Institute on Drug Abuse, National Institutes of Health.

Conflict of interest: none declared.

References

Alam, M., Angelov, S., Stemmler, M., et al. (2015). Neuronal activity of the prefrontal cortex is reduced in rats selectively bred for deficient sensorimotor gating. Prog. Neuropsychopharmacol. Biol. Psychiatry *56*, 174–184.

Allen, N.C., Bagade, S., McQueen, M.B., et al. (2008). Systematic meta-analyses and field synopsis of genetic association studies in schizophrenia: the SzGene database. Nat. Genet. *40*, 827–834.

Barde, Y.A., Edgar, D., and Thoenen, H. (1982). Purification of a new neurotrophic factor from mammalian brain. EMBO J. *1*, 549–553.

Berghuis, P., Dobszay, M.B., Sousa, K.M., et al. (2004). Brain-derived neurotrophic factor controls functional differentiation and microcircuit formation of selectively isolated fast-spiking GABAergic interneurons. Eur. J. Neurosci. *20*, 1290–1306.

Bloodgood, B.L., Sharma, N., Browne, H.A., et al. (2013). The activity-dependent transcription factor NPAS4 regulates domain-specific inhibition. Nature *503*, 121–125.

Braff, D.L., Geyer, M.A., and Swerdlow, N.R. (2001). Human studies of prepulse inhibition of startle: normal subjects, patient groups, and pharmacological studies. Psychopharmacology *156*, 234–258.

Bruns, D., Riedel, D., Klingauf, J., et al. (2000). Quantal release of serotonin. Neuron *28*, 205–220.

Carlson, G.C., Talbot, K., Halene, T.B., et al. (2011). Dysbindin-1 mutant mice implicate reduced fast-phasic inhibition as a final common disease mechanism in schizophrenia. Proc. Natl Acad. Sci. USA *108*, E962–E970.

Chen, X.W., Feng, Y.Q., Hao, C.J., et al. (2008). DTNBP1, a schizophrenia susceptibility gene, affects kinetics of transmitter release. J. Cell Biol. *181*, 791–801.

Daly, K.M., Li, Y., and Lin, D.T. (2015). Imaging the insertion of superecliptic pHluorin-labeled dopamine D2 receptor using total internal reflection fluorescence microscopy. Curr. Protoc. Neurosci. *70*, 5.31.1–5.31.20.

Dean, C., Liu, H., Staudt, T., et al. (2012). Distinct subsets of Syt-IV/BDNF vesicles are sorted to axons versus dendrites and recruited to synapses by activity. J. Neurosci. *32*, 5398–5413.

Dieni, S., Matsumoto, T., Dekkers, M., et al. (2012). BDNF and its pro-peptide are stored in presynaptic dense core vesicles in brain neurons. J. Cell Biol. *196*, 775–788.

Duan, J., Martinez, M., Sanders, A.R., et al. (2007). DTNBP1 (Dystrobrevin binding protein 1) and schizophrenia: association evidence in the 3' end of the gene. Hum. Hered. *64*, 97–106.

Dwivedi, Y., Rizavi, H.S., Conley, R.R., et al. (2003). Altered gene expression of brain-derived neurotrophic factor and receptor tyrosine kinase B in postmortem brain of suicide subjects. Arch. Gen. Psychiatry *60*, 804–815.

Farrell, M.S., Werge, T., Sklar, P., et al. (2015). Evaluating historical candidate genes for schizophrenia. Mol. Psychiatry *20*, 555–562.

Ghosh, A., Carnahan, J., and Greenberg, M.E. (1994). Requirement for BDNF in activity-dependent survival of cortical neurons. Science *263*, 1618–1623.

Gratacos, M., Gonzalez, J.R., Mercader, J.M., et al. (2007). Brain-derived neurotrophic factor Val66Met and psychiatric disorders: meta-analysis of case-control studies confirm association to substance-related disorders, eating disorders, and schizophrenia. Biol. Psychiatry *61*, 911–922.

Green, M.J., Matheson, S.L., Shepherd, A., et al. (2011). Brain-derived neurotrophic factor levels in schizophrenia: a systematic review with meta-analysis. Mol. Psychiatry *16*, 960–972.

Hashimoto, T., Volk, D.W., Eggan, S.M., et al. (2003). Gene expression deficits in a subclass of GABA neurons in the prefrontal cortex of subjects with schizophrenia. J. Neurosci. *23*, 6315–6326.

Henriques, R., Lelek, M., Fornasiero, E.F., et al. (2010). QuickPALM: 3D real-time photoactivation nanoscopy image processing in ImageJ. Nat. Methods *7*, 339–340.

Huang, B., Wang, W., Bates, M., et al. (2008). Three-dimensional super-resolution imaging by stochastic optical reconstruction microscopy. Science *319*, 810–813.

Japha, K., and Koch, M. (1999). Picrotoxin in the medial prefrontal cortex impairs sensorimotor gating in rats: reversal by haloperidol. Psychopharmacology *144*, 347–354.

Ji, Y., Yang, F., Papaleo, F., et al. (2009). Role of dysbindin in dopamine receptor trafficking and cortical GABA function. Proc. Natl Acad. Sci. USA *106*, 19593–19598.

Karege, F., Perret, G., Bondolfi, G., et al. (2002). Decreased serum brain-derived neurotrophic factor levels in major depressed patients. Psychiatry Res. *109*, 143–148.

Kim, Y.K., Lee, H.P., Won, S.D., et al. (2007). Low plasma BDNF is associated with suicidal behavior in major depression. Prog. Neuropsychopharmacol. Biol. Psychiatry *31*, 78–85.

Klamer, D., Svensson, L., Fejgin, K., et al. (2011). Prefrontal NMDA receptor antagonism reduces impairments in pre-attentive information processing. Eur. Neuropsychopharmacol. *21*, 248–253.

Klyachko, V.A., and Jackson, M.B. (2002). Capacitance steps and fusion pores of small and large-dense-core vesicles in nerve terminals. Nature *418*, 89–92.

Kohara, K., Yasuda, H., Huang, Y., et al. (2007). A local reduction in cortical GABAergic synapses after a loss of endogenous brain-derived neurotrophic factor, as revealed by single-cell gene knock-out method. J. Neurosci. *27*, 7234–7244.

Lee, S.A., Kim, S.M., Suh, B.K., et al. (2015). Disrupted-in-schizophrenia 1 (DISC1) regulates dysbindin function by enhancing its stability. J. Biol. Chem. *290*, 7087–7096.

Lessmann, V., and Brigadski, T. (2009). Mechanisms, locations, and kinetics of synaptic BDNF secretion: an update. Neurosci. Res. *65*, 11–22.

Lewis, D.A. (2014). Inhibitory neurons in human cortical circuits: substrate for cognitive dysfunction in schizophrenia. Curr. Opin. Neurobiol. *26*, 22–26.

Lewis, D.A., Hashimoto, T., and Volk, D.W. (2005). Cortical inhibitory neurons and schizophrenia. Nat. Rev. Neurosci. *6*, 312–324.

Li, W., Zhang, Q., Oiso, N., et al. (2003). Hermansky-Pudlak syndrome type 7 (HPS-7) results from mutant dysbindin, a member of the biogenesis of lysosome-related organelles complex 1 (BLOC-1). Nat. Genet. *35*, 84–89.

Li, X., Rubio, F.J., Zeric, T., et al. (2015). Incubation of methamphetamine craving is associated with selective increases in expression of Bdnf and trkb, glutamate receptors, and epigenetic enzymes in cue-activated fos-expressing dorsal striatal neurons. J. Neurosci. *35*, 8232–8244.

Li, Y., Roy, B.D., Wang, W., et al. (2012a). Imaging pHluorin-tagged receptor insertion to the plasma membrane in primary cultured mouse neurons. J. Vis. Exp. pii: 4450.

Li, Y., Roy, B.D., Wang, W., et al. (2012b). Identification of two functionally distinct endosomal recycling pathways for dopamine D_2 receptor. J. Neurosci. *32*, 7178–7190.

Lieberman, J.A., Stroup, T.S., McEvoy, J.P., et al. (2005). Effectiveness of antipsychotic drugs in patients with chronic schizophrenia. N. Engl. J. Med. *353*, 1209–1223.

Lin, D.T., Makino, Y., Sharma, K., et al. (2009). Regulation of AMPA receptor extrasynaptic insertion by 4.1N, phosphorylation and palmitoylation. Nat. Neurosci. *12*, 879–887.

Lu, B. (2003). BDNF and activity-dependent synaptic modulation. Learn. Mem. *10*, 86–98.

Martinotti, G., Di Iorio, G., Marini, S., et al. (2012). Nerve growth factor and brain-derived neurotrophic factor concentrations in schizophrenia: a review. J. Biol. Regul. Homeost. Agents *26*, 347–356.

Nagahara, A.H., Merrill, D.A., Coppola, G., et al. (2009). Neuroprotective effects of brain-derived neurotrophic factor in rodent and primate models of Alzheimer's disease. Nat. Med. *15*, 331–337.

Ouagazzal, A.M., and Meziane, H. (2012). Acoustic startle reflex and prepulse inhibition. Curr. Protoc. Mouse Biol. *2*, 25–35.

Papaleo, F., Yang, F., Garcia, S., et al. (2012). Dysbindin-1 modulates prefrontal cortical activity and schizophrenia-like behaviors via dopamine/D2 pathways. Mol. Psychiatry *17*, 85–98.

Park, H., and Poo, M.M. (2013). Neurotrophin regulation of neural circuit development and function. Nat. Rev. Neurosci. *14*, 7–23.

Perry, W., Minassian, A., Feifel, D., et al. (2001). Sensorimotor gating deficits in bipolar disorder patients with acute psychotic mania. Biol. Psychiatry *50*, 418–424.

Perry, W., Minassian, A., Lopez, B., et al. (2007). Sensorimotor gating deficits in adults with autism. Biol. Psychiatry *61*, 482–486.

Pezze, M., McGarrity, S., Mason, R., et al. (2014). Too little and too much: hypoactivation and disinhibition of medial prefrontal cortex cause attentional deficits. J. Neurosci. *34*, 7931–7946.

Powell, S.B., Zhou, X., and Geyer, M.A. (2009). Prepulse inhibition and genetic mouse models of schizophrenia. Behav. Brain Res. *204*, 282–294.

Purcell, S.M., Moran, J.L., Fromer, M., et al. (2014). A polygenic burden of rare disruptive mutations in schizophrenia. Nature *506*, 185–190.

Regier, D.A., Narrow, W.E., Rae, D.S., et al. (1993). The de facto US mental and addictive disorders service system. Epidemiologic catchment area prospective 1-year prevalence rates of disorders and services. Arch. Gen. Psychiatry *50*, 85–94.

Rios, M., Fan, G., Fekete, C., et al. (2001). Conditional deletion of brain-derived neurotrophic factor in the postnatal brain leads to obesity and hyperactivity. Mol. Endocrinol. *15*, 1748–1757.

Saggu, S., Cannon, T.D., Jentsch, J.D., et al. (2013). Potential molecular mechanisms for decreased synaptic glutamate release in dysbindin-1 mutant mice. Schizophr. Res. *146*, 254–263.

Sanders, A.R., Duan, J., Levinson, D.F., et al. (2008). No significant association of 14 candidate genes with schizophrenia in a large European ancestry sample: implications for psychiatric genetics. Am. J. Psychiatry *165*, 497–506.

Schizophrenia Working Group of the Psychiatric Genomics, C. (2014). Biological insights from 108 schizophrenia-associated genetic loci. Nature *511*, 421–427.

Schmitt, A., Malchow, B., Hasan, A., et al. (2014). The impact of environmental factors in severe psychiatric disorders. Front. Neurosci. *8*, 19.

Skarnes, W.C., Rosen, B., West, A.P., et al. (2011). A conditional knockout resource for the genome-wide study of mouse gene function. Nature *474*, 337–342.

Stefansson, H., Meyer-Lindenberg, A., Steinberg, S., et al. (2014). CNVs conferring risk of autism or schizophrenia affect cognition in controls. Nature *505*, 361–366.

Straub, R.E., Jiang, Y., MacLean, C.J., et al. (2002). Genetic variation in the 6p22.3 gene DTNBP1, the human ortholog of the mouse dysbindin gene, is associated with schizophrenia. Am. J. Hum. Genet. *71*, 337–348.

Sullivan, P.F., Lin, D., Tzeng, J.Y., et al. (2008). Genomewide association for schizophrenia in the CATIE study: results of stage 1. Mol. Psychiatry *13*, 570–584.

Sun, J., Kuo, P.H., Riley, B.P., et al. (2008). Candidate genes for schizophrenia: a survey of association studies and gene ranking. Am. J. Med. Genet. B Neuropsychiatr. Genet. *147B*, 1173–1181.

Swerdlow, N.R., Benbow, C.H., Zisook, S., et al. (1993). A preliminary assessment of sensorimotor gating in patients with obsessive compulsive disorder. Biol. Psychiatry *33*, 298–301.

Swerdlow, N.R., and Geyer, M.A. (1998). Using an animal model of deficient sensorimotor gating to study the pathophysiology and new treatments of schizophrenia. Schizophr. Bull. *24*, 285–301.

Swerdlow, N.R., Geyer, M.A., and Braff, D.L. (2001a). Neural circuit regulation of prepulse inhibition of startle in the rat: current knowledge and future challenges. Psychopharmacology *156*, 194–215.

Swerdlow, N.R., Karban, B., Ploum, Y., et al. (2001b). Tactile prepuff inhibition of startle in children with Tourette's syndrome: in search of an 'fMRI-friendly' startle paradigm. Biol. Psychiatry *50*, 578–585.

Swerdlow, N.R., Paulsen, J., Braff, D.L., et al. (1995). Impaired prepulse inhibition of acoustic and tactile startle response in patients with Huntington's disease. J. Neurol. Neurosurg. Psychiatry *58*, 192–200.

Swerdlow, N.R., Weber, M., Qu, Y., et al. (2008). Realistic expectations of prepulse inhibition in translational models for schizophrenia research. Psychopharmacology *199*, 331–388.

Szekeres, G., Juhasz, A., Rimanoczy, A., et al. (2003). The C270T polymorphism of the brain-derived neurotrophic factor gene is associated with schizophrenia. Schizophr. Res. *65*, 15–18.

Talbot, K. (2009). The sandy (sdy) mouse: a dysbindin-1 mutant relevant to schizophrenia research. Prog. Brain Res. *179*, 87–94.

Talbot, K., Eidem, W.L., Tinsley, C.L., et al. (2004). Dysbindin-1 is reduced in intrinsic, glutamatergic terminals of the hippocampal formation in schizophrenia. J. Clin. Invest. *113*, 1353–1363.

Tang, T.T., Yang, F., Chen, B.S., et al. (2009). Dysbindin regulates hippocampal LTP by controlling NMDA receptor surface expression. Proc. Natl Acad. Sci. USA *106*, 21395–21400.

Vilella, E., Costas, J., Sanjuan, J., et al. (2008). Association of schizophrenia with DTNBP1 but not with DAO, DAOA, NRG1 and RGS4 nor their genetic interaction. J. Psychiatr. Res. *42*, 278–288.

Weickert, C.S., Hyde, T.M., Lipska, B.K., et al. (2003). Reduced brain-derived neurotrophic factor in prefrontal cortex of patients with schizophrenia. Mol. Psychiatry *8*, 592–610.

Weickert, C.S., Rothmond, D.A., Hyde, T.M., et al. (2008). Reduced DTNBP1 (dysbindin-1) mRNA in the hippocampal formation of schizophrenia patients. Schizophr. Res. *98*, 105–110.

Woo, T.U., Whitehead, R.E., Melchitzky, D.S., et al. (1998). A subclass of prefrontal gamma-aminobutyric acid axon terminals are selectively altered in schizophrenia. Proc. Natl Acad. Sci. USA *95*, 5341–5346.

Xia, X., Lessmann, V., and Martin, T.F. (2009). Imaging of evoked dense-core-vesicle exocytosis in hippocampal neurons reveals long latencies and kiss-and-run fusion events. J. Cell Sci. *122*, 75–82.

Yuan, Q., Yang, F., Xiao, Y., et al. (2015). Regulation of brain-derived neurotrophic factor exocytosis and gamma-aminobutyric acidergic interneuron synapse by the schizophrenia susceptibility gene dysbindin-1. Biol. Psychiatry pii: S0006-3223(15)00684-8.

Zhang, W., Peterson, M., Beyer, B., et al. (2014). Loss of MeCP2 from forebrain excitatory neurons leads to cortical hyperexcitation and seizures. J. Neurosci. *34*, 2754–2763.

Zhang, Z., Wu, Y., Wang, Z., et al. (2011). Release mode of large and small dense-core vesicles specified by different synaptotagmin isoforms in PC12 cells. Mol. Biol. Cell *22*, 2324–2336.